

On the family “g” of the restricted three-body problem

Martin Lara and Ryan P. Russell

Real Observatorio de la Armada, 11110 San Fernando

Abstract

The family g of periodic orbits of the Restricted Three-body Problem —planar, direct, periodic orbits around the smaller primary— is of interest in astrodynamics. Specifically, in the case of natural planetary satellites it is known that it provides stable, egg-shaped, periodic orbits close to the natural satellite, which could be used for a variety of applications. In the limit case of Hill the family g no longer provides egg-shaped orbits, which now pertain to the family g' that bifurcates from g at a certain value of the Jacobi constant. We investigate the influence of the mass ratio between the primaries in the behavior of direct periodic orbits of the Restricted Three-body Problem, and find that different parts of the family g are linked through new families of three-dimensional periodic orbits. Further, we find that the family g' is a limiting case of the family g , where the two parts made of egg-shaped orbits match exactly.

1 Introduction

The existence of liquid water in some icy moons, pointed by the recent NASA’s Cassini finding of a cloud of oxygen exuded by Enceladus and the prior NASA’s Galileo discovery of a briny ocean under the surface of Europa, motivate strong scientific interest in new missions to planetary satellites. Old results from Celestial Mechanics are at the disposal of astrodynamacists for their mission design studies, where the computation of periodic orbits of the Restricted Three-body Problem (RTBP) play a role in determining transfers, stability regions, or even the science orbit [10, 12, 13, 15].

Among the overwhelming amount of results on periodic orbits of the RTBP, Szebeheley’s book [16] and Hénon’s original papers [5, 6, 7, 8, 9] remain as fundamental references on the topic. The basic periodic orbit families of the RTBP start as small retrograde oscillations around the five Lagrangian points, and retrograde and direct oscillations around each primary. After Strömberg, the basic families are named alphabetically corresponding the letter g to the family originating from small direct oscillations around the smaller

primary. Strömberg and coworkers considered the equal mass case that is primarily of interest in stellar dynamics. Other authors studied mass ratios between the primaries that are of interest in the solar system, for which they used different nomenclatures. Thus, for instance, Broucke [1] computed two “different” families of direct periodic orbits around the Moon that he named H_1 and H_2 , yet he speculated that both families should be part of a type- g earth-Moon family. Analogously, Szebehely [16] classifies Darwin’s families A, B, and C of satellites as parts of a type- g family of Darwin’s “sun-Jupiter” system.

Despite planar stability regions of direct motion around the primaries are known to be smaller than those of retrograde motion [6], a surprising recent result [12, 15] shows that stability regions of direct motion close to the smaller primary can be larger in three-dimensions than similar regions of retrograde motion. The stability regions in three-dimensions computed in [12] originate from planar direct motion around the smaller primary. Then, we feel compelled to revisit previous results on families of periodic orbits that originate from small, planar, direct oscillations around the smaller primary; more specifically to those parts of these families with orbits that remain close to the smaller primary.

We continue several families of three-dimensional periodic orbits that bifurcate vertically from the family g close to the smaller primary, and find that they connect different parts of the family g through three-dimensional space. We find this behavior in Strömberg’s case of equal masses, but we also find these kind of connections linking Darwin’s families A, B, and C, and Broucke’s families H_1 and H_2 , which supports the belief that they are parts of the same family g . For very small mass ratios, such as the case of many planetary satellites, we also find that these three dimensional connections are very similar to the connections of the families g and g' computed by Michalodimitrakis [14] for the Hill problem.

The computations of this paper show that for decreasing values of the mass ratio between the primaries the two parts of the family g that are made of stable periodic orbits close to the smaller primary, get closer and closer to each other in terms of the Jacobi constant values, until they exactly match for the Hill problem. Therefore, the family g' is a limit case of the family g produced by the symmetries of the Hill model.

Other families of three-dimensional periodic orbits that bifurcate vertically from the family g are found to connect direct and retrograde motion around the smaller primary in the case of equal masses, which was a known result for higher order resonances in the Jupiter-Europa system [11]. Finally, we find practical application for a three-dimensional g family orbit at Enceladus as a stable science orbit with global ground visibility.

For completeness, we summarize in the appendix the well known equations of the RTBP and recall usual definitions of stability indices.

2 The family g

The ratio of the smaller primary to the total mass of the system is the mass parameter μ , which ranges from the Copenhagen category ($\mu = 1/2$, equal masses) to the limit case of Hill ($\mu \rightarrow 0$). We use a reference system centered on the smaller primary, which we call “smaller” even in the case of equal masses.

Starting from small, planar, direct, stable oscillations around the smaller primary, the family g presents an intricate behavior passing through different collisions, suffering from reflections, and changing from stability to instability at different values of the Jacobi constant. These complications motivate phrases like Henon’s ([5], p. 11) “*La courbe de stabilité est très compliquée [...] et n’a pas été dessinée en entier*”, or Broucke’s ([1], p. 71) “*It is likely that, if one were to continue family H_1 or the two open ends of H_2 , some junction between H_1 and H_2 would be found*”.

2.1 Equal masses

The family g starts with almost circular orbits that soon change to ovals. After different phases with orbits of exotic shapes the orbits become ovals again (see [16], pp. 466–470). Remarkably, ovals of different parts of the family g are relatively close in terms of the Jacobi constant.

Figure 1 shows the part of the family g that is of current interest. The right plot of the figure shows sample stable and unstable ovals, while the left plot presents the horizontal and vertical stability curves, where we can see several of the many critical points identified in [8]. Specifically, in the left plot of Fig. 1 we find: reflections $g1$, $g2$, $g14$; horizontal, period doubling bifurcations $g3$, $g15$; vertical, period doubling bifurcations $g1v$, $g2v$, $g11v$, $g12v$, $g13v$, and $g14v$; and the vertical bifurcation g_23v .

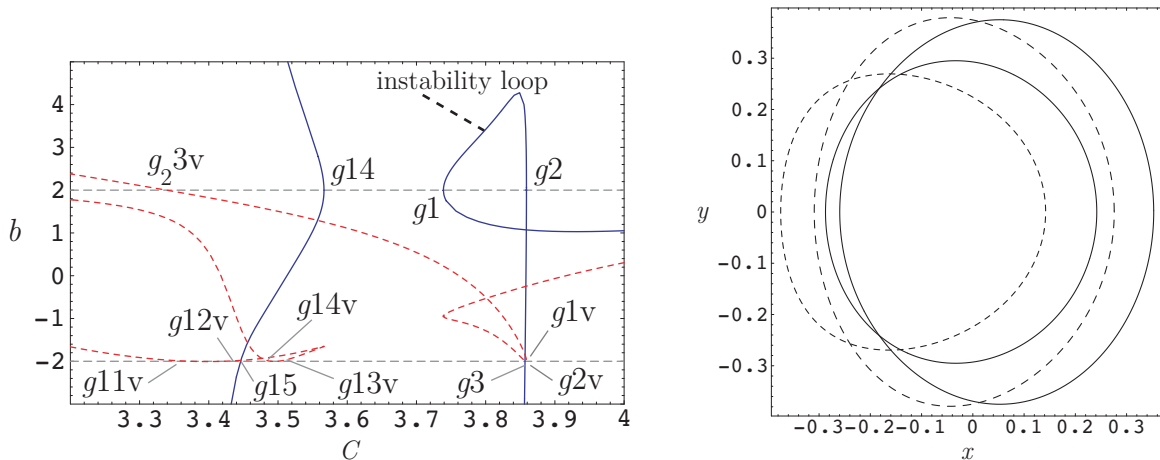


Figure 1.— Family g of the Copenhagen category. Left: Horizontal (full line) and vertical (dashed) stability curves. Right: Sample stable (full line) and unstable (dashed) periodic orbits for $C = 3.8$, the smaller ones, and $C = 3.54$.

The continuation of the family g from the ovals that first occur around $C = 3.8$ to those around $C = 3.5$ is tedious to follow because of the collisions and reflections in between. However, as an alternative route, we find a shortcut by computing the families of three-dimensional periodic orbits that bifurcate from Henon's points $g1v$ and $g2v$, which we call families $g1v$ and $g2v$, respectively.

Thus, the family $g1v$ bifurcates from g at $C = 3.8579$ in a vertical, period doubling bifurcation of Henon's type D_v [8] —bifurcation orbit with initial conditions $(x, 0, 0, 0, \dot{y}, \dot{z} = \epsilon)$ — and exists for decreasing values of the Jacobi constant. It is made of unstable orbits that change to complex instability in the interval $3.82204 > C > 3.5022$. The family reflects over itself at $C = 3.31099$ and continues for increasing values of the Jacobi constant until its termination at $C = 3.37345$ (Henon's point $g11v$) in a period doubling bifurcation of the family g , again of the type D_v . Figure 2 shows the stability curves b_1 and b_2 (left plot) and two sample periodic orbits close to the bifurcations (right plot). Note the inverse hyperbolic sine scale used for the stability curves. For the complex unstable orbits, b_1 is always the conjugate of b_2 [2], thus only the positive branch is illustrated (dotted line in the left plot of Fig. 2).

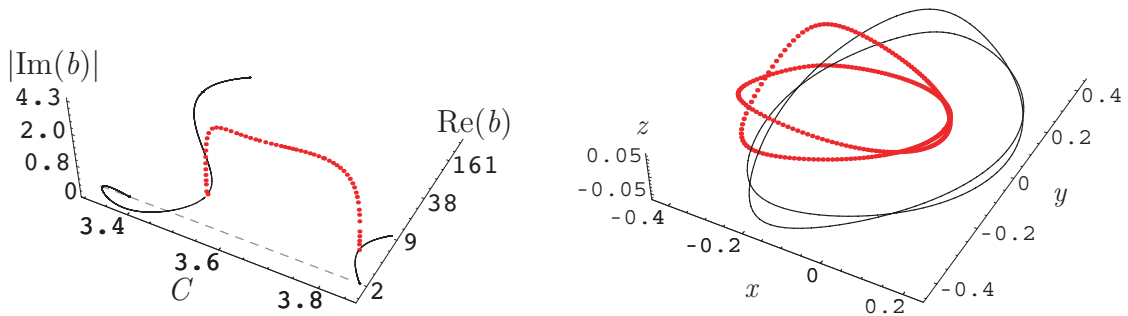


Figure 2.— Family $g1v$ of the Copenhagen category. Stability curves and sample orbits.

The behavior of the family $g2v$ is very similar to the previous one, although both period doubling bifurcations from the family g are now of type A_v —bifurcation orbit with initial conditions $(x, 0, z = \epsilon, 0, \dot{y}, 0)$. It starts at $C = 3.85839$, suffers a reflection at $C = 3.28772$, and ends at $C = 3.42236$ (Henon's point $g12v$). It is made of unstable orbits, but now we do not find the complex instability region. The left plot of Fig. 3 shows the stability curve corresponding to the b_2 stability index of the family $g2v$ jointly with the vertical stability curve of the family g . The index b_1 varies in the range $7.57 \leq b_1 \leq 147.3$ and is not presented. Sample orbits of the family $g2v$ close to its bifurcations from g are presented in the right plot of Fig. 3, where the higher value of the Jacobi constant corresponds to the smaller size of the orbit.

We also find other three-dimensional connections between planar orbits by computing

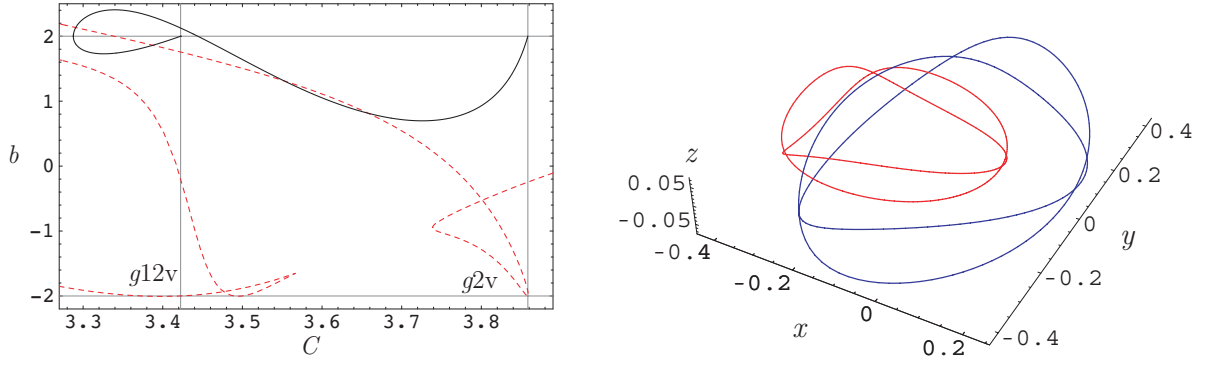


Figure 3.— Family $g2v$ of the Copenhagen category. Left: b_2 stability curve of family $g2v$ (full line) and vertical stability curve of the family g (dashed); the vertical lines mark the bifurcation points $g2v$, $g12v$. The range of ordinates presented does not include the high b_1 values. Right: Sample orbits close to the bifurcations.

the vertically bifurcated families at $C = 3.49986$ and $C = 3.4895$ (Henon's points $g13v$ and $g14v$). These new families do not link two parts of the same family, but they connect direct and retrograde motion around the smaller primary. The family $g13v$ bifurcates from the plane in a type A_v period doubling bifurcation and ends at $C = 1.47930$ on a four-fold periodic orbit of the family f (retrograde motion around the smaller primary). Similarly, the family $g14v$ bifurcates from the plane in a type D_v period doubling bifurcation, and ends at $C = 1.47936$ on a four-fold periodic orbit of the family f . Despite the orbits of both families are very similar in shape, the family $g14v$ is made of unstable orbits while $g13v$ enjoys two regions of stability for $C < 1.63864$ and $C > 2.86972$. Figure 4 shows the stability curves of the families $g13v$ and $g14v$. Some sample stable orbits of the family $g13v$ are presented in Fig. 5.

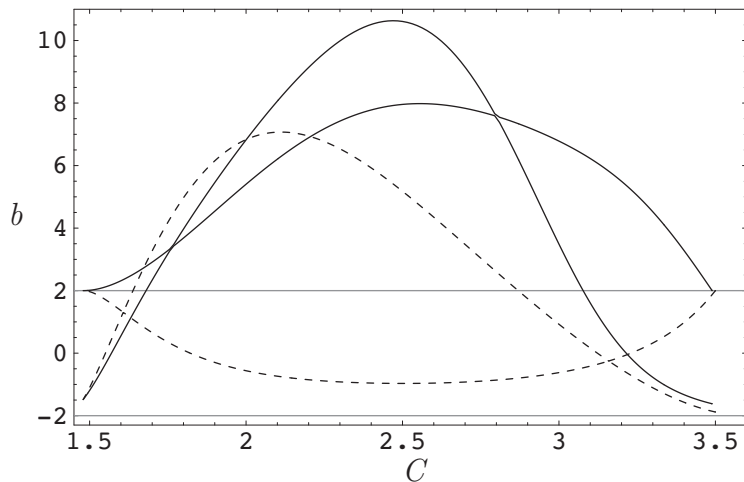


Figure 4.— Stability curves of the families $g13v$ (dashed lines) and $g14v$ (full lines).

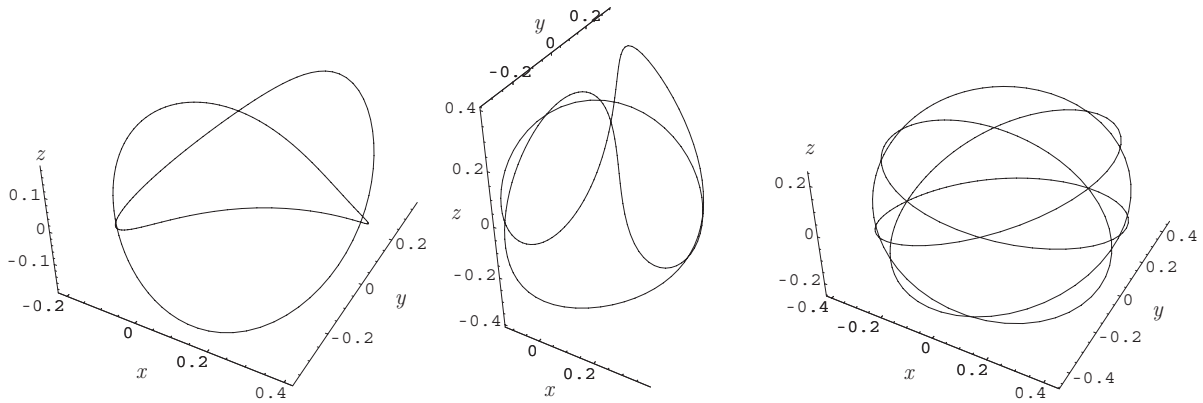


Figure 5.— Stable orbits of the family $g13v$ for $C = 3.4$ (left), 2.9 (center), and 1.6 (right).

2.2 Darwin's and Broucke's computations

Darwin [3] considers a mass parameter $\mu = 1/11$ for a “sun-Jupiter” system.¹ A dramatic difference between Darwin's family A and Strömngren's family g is that direct orbits around the smaller primary do not find the first reflection (see Fig. 6 in comparison to Fig. 1). From our computations, we find that the region of (mild) instability in Fig. 1 between the two first reflections at the critical points $g1$ and $g2$ reduces in size for decreasing values of the mass parameter until it disappears at $\mu \approx 0.11$. Therefore, the loop of instability does not occur for Darwin's family A: the extrema in C at $g1$ and $g2$ (critical points of Henon's [6] type 1) do not exist any longer, and the family A remains stable until the first vertical bifurcation $g1v$, of type D_v , that occurs at $C = 3.55241$. The orbits of the family A immediately return to stability at $C = 3.55187$ in another vertical period doubling bifurcation $g2v$, now of type A_v . Note that, using Henon's notation, the first critical point of Darwin's family A is named $g1v$, but contrary to the Copenhagen category it occurs for a value of the Jacobi constant higher than the value where $g2v$ occurs. At $C = 3.55074$ the orbits become unstable again after a horizontal period doubling bifurcation, and soon approach to a collision orbit.

Rather than continue Darwin's family A through collisions and reflections, we instead compute the vertically bifurcated family $g1v$, and present the stability curves in the left plot of Fig. 7. As illustrated in the right plot of Fig. 7, the sun-Jupiter family $g1v$ ends on a planar, type A_v period doubling bifurcation orbit from Darwin's family B at $g11v$, $C = 3.2729$. Similarly to the family $g1v$ of the Strömngren's case of equal masses, the sun-Jupiter family $g1v$ has large areas of complex instability. However, contrary to the case of equal masses where the family $g1v$ is always unstable, the sun-Jupiter family $g1v$

¹Note that the value $\mu \approx 0.1$ for Darwin's Sun-Jove system is about two orders of magnitude over the real value $\mu \approx 0.001$ of the sun-Jupiter system. Consequently, Szebehely classifies Darwin's case in the Copenhagen category.

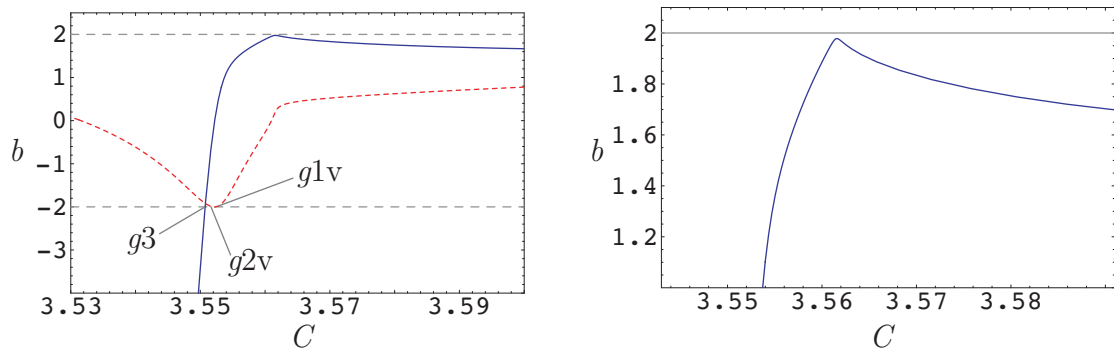


Figure 6.— Darwin’s family A. Left: Horizontal (full line) and vertical (dashed) stability curves. Right: Magnification.

enjoys a small region of stability between its bifurcation from the family A at $C = 3.55241$ and the change to complex instability at $C = 3.54172$.

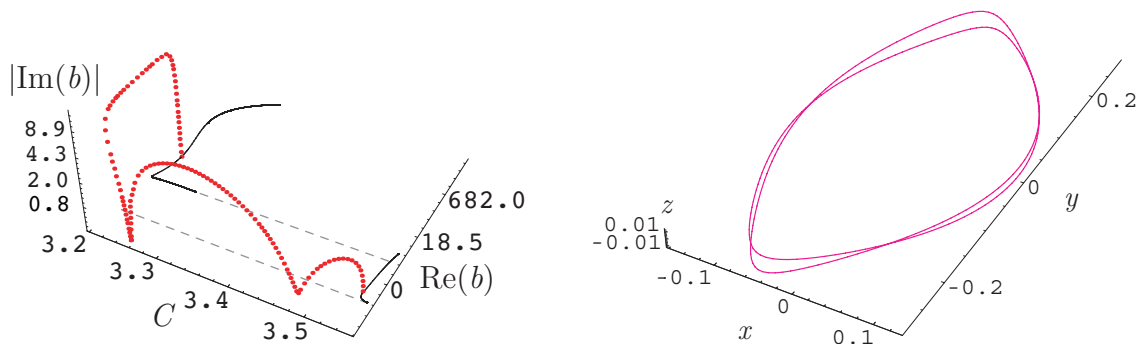


Figure 7.— Three-dimensional connection of Darwin’s families A and B. Left: Stability curves. Right: highly unstable periodic orbit close to the termination onto the family B.

The continuation of Darwin’s family B for increasing values of the Jacobi constant shows that it reflects over itself at $C = 3.49211$ and continues with orbits of the family C (see Fig. 8). Therefore, we can conclude with Szebehely [16], p. 492, that “*Darwin’s families A, B, and C of satellites correspond to a part of Strömgen’s Class (g)*”.

Note that we named the critical points in Fig. 8 analogously to corresponding ones in the case of equal masses. However, we did not continue the planar families A and B through collisions and reflections until finding the presumed junction. Therefore, one should not consider the indices as an enumeration of critical points. Table 1 provides the characteristics of these critical orbits, where b means b_h except for orbits $g3$, $g14$, and $g15$, where b is b_v .

Similarly to the case of equal masses, we find a second connection between different parts of the sun-Jupiter family g (or Darwin’s families C and B). However, contrary to the case of equal masses, this new connection is not reached through the sun-Jupiter family $g2v$, but it is established by the family of three-dimensional periodic orbits that vertically

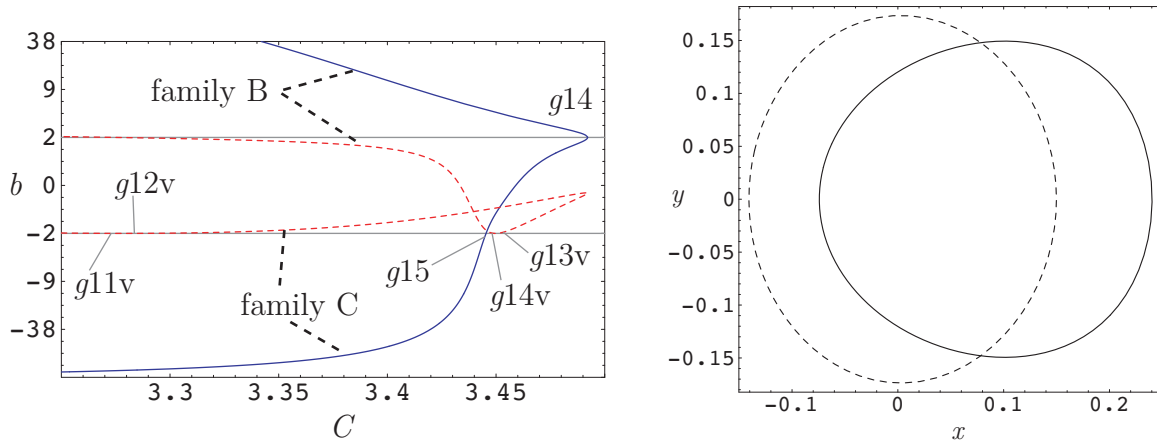


Figure 8.— Darwin’s families B and C. Left: Horizontal (full line) and vertical (dashed) stability curves. Right: Two sample stable (full line) and unstable (dashed) orbits for $C = 3.46$.

Orbit	x	C	Period	b
$g1v$	-0.2435991439849617	3.552410898304	1.8493709733738	0.18354733
$g2v$	-0.2455174512342443	3.551869991020	1.8968265295139	-0.37276085
$g3$	-0.2484286120350057	3.550737367633	1.9836232812507	-1.92094641
$g11v$	-0.1562486451302664	3.272898336713	2.9529359920457	117.877474
$g12v$	-0.1570471865924994	3.284532038939	2.8803898003163	99.7640602
$g14$	-0.1180857532701786	3.492114811420	1.5282345073578	-0.23555266
$g13v$	0.2651671916648681	3.450426595805	2.4310924660528	-0.86763844
$g14v$	0.2689765674982433	3.449074178436	2.5079655829120	-1.07197976
$g15$	0.2788037226766065	3.445400246793	2.7570329211262	-0.17941511

Table 1.— Some critical orbits of the sun-Jupiter family g ($y = \dot{x} = 0$).

bifurcates from Darwin’s family C at the critical point $g13v$.

Thus, the sun-Jupiter family $g13v$ bifurcates from Darwin’s family C at a Jacobi constant value $C = 3.45043$ in a type D_v period doubling bifurcation. It starts with stable orbits that change to complex instability at $C = 3.38533$. At $C = 3.1336$ the orbits become stable, change again to complex instability at $C = 3.106$, and to instability at $C = 3.07466$. Then, a reflection immediately occurs and, for increasing values of the Jacobi constant, the sun-Jupiter family $g13v$ continues with unstable orbits until its termination at $C = 3.28453$ in a type A_v , period doubling bifurcation from the family B.

Figure 9 shows the stability curves of the sun-Jupiter families $g1v$ and $g13v$ jointly with those of the family g . A two-dimensional projection ($C, \text{Re}(b)$) is provided where, for clarity, the real part of complex stability indices is not presented; therefore, $\text{Re}(b) \equiv b$. Note the region of stability of the family $g13v$ in $3.106 < C < 3.1336$ (the small closed

curve at the left bottom corner of the left plot of Fig. 9); the right plot of Fig. 9 shows a sample stable periodic orbit in this region.

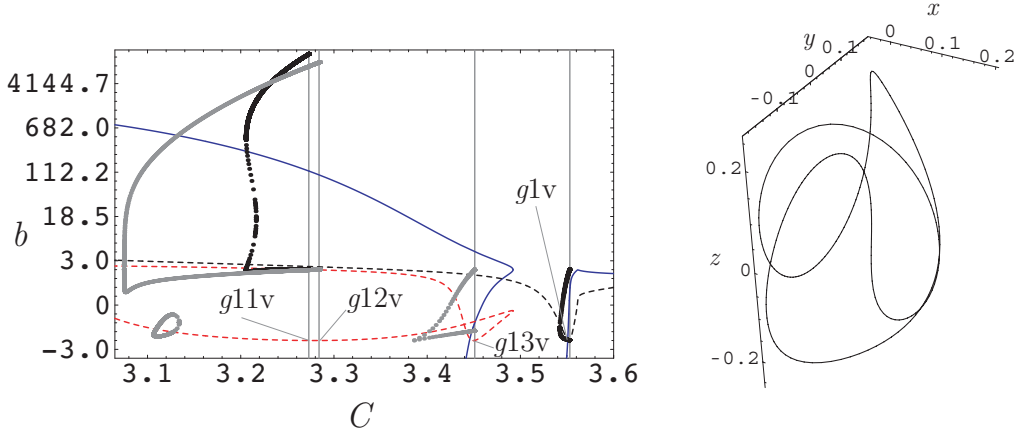


Figure 9.— Left: Stability curves of Darwin’s families A, B, and C (full and dashed lines), and its connecting families $g1v$ (black dotted) and $g13v$ (gray dotted); vertical lines mark the bifurcations of $g1v$ and $g13v$. Right: Stable orbit of $g13v$ for $C = 3.126$. See text for further explanation.

The stability curves of the sun-Jupiter families $g2v$ and $g14v$ are presented in the left plot of Fig. 10. The family $g2v$ bifurcates from Darwin’s family A in a type A_v period doubling bifurcation at $C = 3.55187$, and is generally made of unstable orbits with two regions of complex instability in $2.24169 < C < 2.54898$ and $3.02395 < C < 3.05267$. However, we find two regions of stability in $2.54898 < C < 2.66915$ and $3.00734 < C < 3.02395$. The right plot of Fig. 10 shows a sample stable orbit.

We do not continue the family $g2v$ until its termination. It seems to exist for decreasing values of the Jacobi constant with orbits of increasing size and instability. A similar behavior is found for the sun-Jupiter system family $g14v$, however we always find instability for the computed orbits.

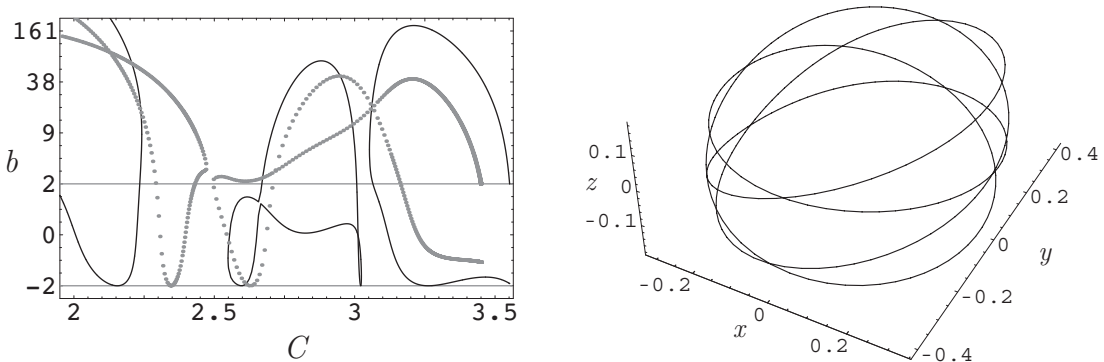


Figure 10.— Stability curves of the sun-Jupiter families $g2v$ (full lines) and $g14v$ (dotted lines). Right: Stable orbit of the family $g2v$ for $C = 2.6$.

Similar results to those of the sun-Jupiter case are found for the Lunar RTBP studied by Broucke [1], who considers a mass parameter $\mu = 0.012155 \approx 1/82.27$ for the earth-Moon system and names H_1 and H_2 —analogous to Darwin’s families B and C respectively— the families of direct periodic orbits he computed around the Moon. Again, we find an earth-Moon family $g1v$ of three-dimensional periodic orbits that bifurcates at $C = 3.18511$ from H_1 and ends at $C = 3.113$ onto H_2 , smoothly connecting Broucke’s families H_1 and H_2 . We also find an earth-Moon family $g13v$ that bifurcates from H_2 at $C = 3.17098$ and ends on H_2 at $C = 3.11448$, thus connecting two different parts of the family H_2 . Figure 11 shows the stability curves of H_1 , H_2 —which we do not continue through collisions and reflections— and the connecting families $g1v$ and $g13v$. Again, we only present the parts of the stability b_1 and b_2 curves of the $g1v$ and $g13v$ families with real stability indices. Note that, as in the sun-Jupiter case, the orbits of $g1v$ and $g13v$ enjoy stability before changing to complex instability, now at $C = 3.17996$ and $C = 3.15928$ respectively.

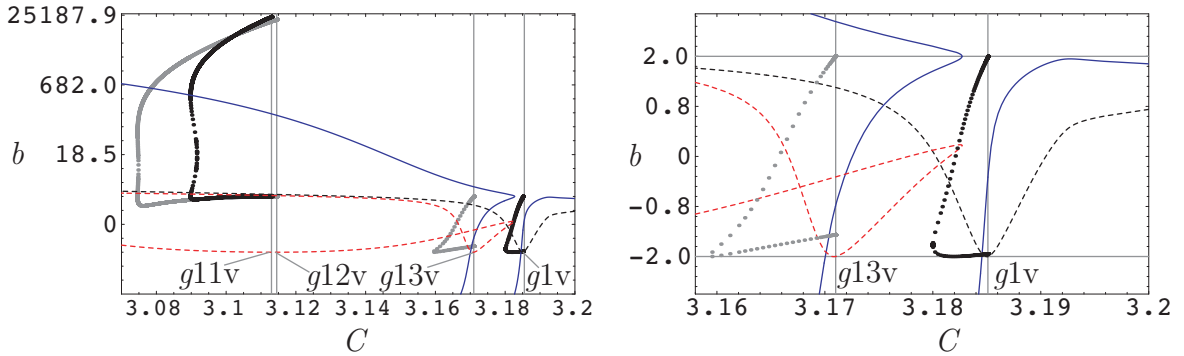


Figure 11.— Left: Stability curves b_h (full line) and b_v (dashed) of families H_1 and H_2 , and its connections $g1v$ (black, dotted) and $g13v$ (gray, dotted) bifurcating at the vertical lines. Right: Magnification on the regions of stability of $g1v$ and $g13v$.

Continuing, we find the earth-Moon families $g2v$ and $g14v$ that bifurcate respectively from H_1 at $C = 3.18491$ and from H_2 at $C = 3.17069$ in two type A_v period doubling bifurcations. These families also show a similar behavior to the sun-Jupiter case and we do not provide the stability curves. The orbits are generally unstable but we can find again stable orbits in the case of $g2v$. The characteristics of Broucke’s mentioned vertical critical orbits are given in Table 2, where $b_v = -2$ always.

2.3 The case of Europa

A much smaller mass parameter applies to a host of other planet-satellite systems. Thus, for instance, $\mu = 2.5 \times 10^{-5}$ for the Jupiter-Europa system. For such small ratios between the primaries either the RTBP or the Hill problem are good models to approximate the real dynamics. When using Hill’s model the family g finds a bifurcation of a new

Orbit	x	C	Period	b_h
$g1v$	-0.1276737432187769	3.185108386266	1.9531534239966	-0.29086064
$g2v$	-0.1288574555922996	3.184913314810	2.0092982280377	-0.72831954
$g11v$	-0.0750867380106130	3.112998766162	2.9548132818750	152.482084
$g12v$	-0.0754072134664140	3.114478718988	2.9214458245635	141.495545
$g13v$	0.1340483871267902	3.170979187720	2.2535326036338	-0.78366577
$g14v$	0.1356854966891561	3.170686700408	2.3237569650483	-1.03818310

Table 2.— Some vertical critical orbits of the earth-Moon family g ($y = \dot{x} = 0$).

family g' of planar, direct periodic orbits that starts with egg-shaped orbits [7]. Due to the symmetries of the Hill problem, there are two families g' each one made of orbits that are symmetric of corresponding orbits of the other family g' with respect to the origin.

Figure 12 shows the vertical and horizontal stability curves of the families g and g' of the Hill problem [9] and the vertical critical orbits of family g and both branches of family g' that are the ends of the bridges of three-dimensional periodic orbits linking the families. The three-dimensional connections of both g' branches of Hill's limiting case with the family g were originally computed by Michalodimitrakis (families $g1v$ and $g'2v$ of [14]). Contrary to [14], where instability is found for all the orbits of the family $g1v$, similarly to the computed cases of the RTBP we find a region of stability before the change to complex instability.

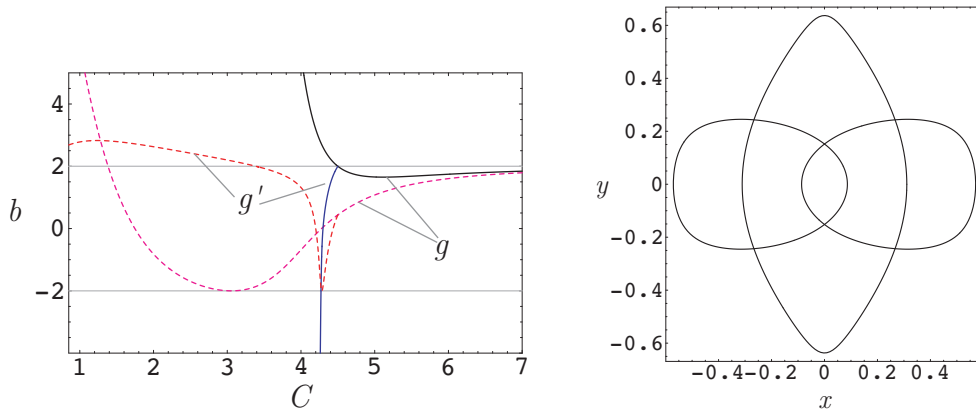


Figure 12.— Left: Vertical (full line) and horizontal (dashed) stability curves of the families g and g' of the Hill problem. Right: critical bifurcation orbits where the family $g1v$ intersects with the family g (oval orbit) and the families g' (egg-shaped orbits).

The behavior of the family of planar, direct, periodic orbits around Europa in the RTBP is analogous to Darwin's and Broucke's cases, and we find again connections of vertical critical orbits of the Jupiter-Europa family g by means of new families of three-dimensional periodic orbits. Figure 13 shows the vertical and horizontal stability curves

of the family g in the Jupiter-Europa RTBP. We note that the left plots of Figs. 12 and 13 are very similar. However, as we see in the magnification in the right plot of Fig. 13, the family g' does not exist in the Jupiter-Europa RTBP. Instead, the two distinct parts of the family g that are made of egg-shaped, direct, periodic orbits are very close to each other in terms of the Jacobi constant. Therefore, from the computations in this paper we see that for decreasing values of the mass parameter μ of the RTBP two parts of the family g get closer and closer to each other in terms of the Jacobi constant values until they exactly match for the Hill problem.

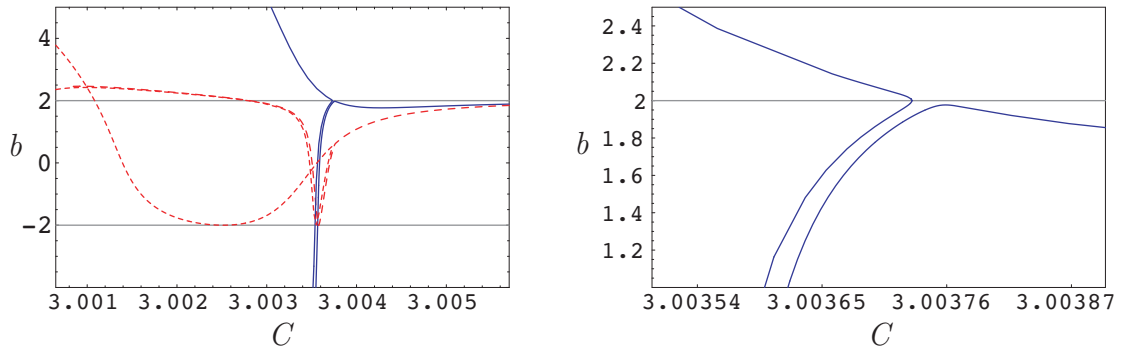


Figure 13.— Left: family g of the Jupiter-Europa system. Right: Magnification.

The gap separating the two distinct branches illustrated on the right side of Fig. 13 is appreciated in the (C, x_0) space for the Earth-Moon case on pg. 89 of [1] and for the Jupiter-Europa case in [15].

2.4 One application to Enceladus

The bifurcation of families of three-dimensional orbits is not limited to simple period or period doubling bifurcations. Other families of higher-resonant periodic orbits bifurcate with multiple periods from the simple families [6]. The multiple period, vertical bifurcations of the family g could provide stability regions of interest for a science mission around a planetary satellite [12]. We find an application for the observation of Enceladus in the family that bifurcates vertically from the family g of the Saturn-Enceladus system after 9 revolutions of the orbiter in 2 revolutions of Enceladus around Saturn.

Figure 14 shows the stability curves of the 9:2 vertical family. Thus, starting from planar, direct, egg-shaped orbits of the family g , decreasing variations of the Jacobi constant produce three-dimensional periodic orbits of increasing z distance with $b_2 \approx 2$ and $|b_1| < 2$. The family finds a reflection in the Jacobi constant at $C = 3.000118$ after which the orbits are clearly stable. The continuation for increasing values of C finds a change to complex instability at $C = 3.000123$ (dotted line), and then to instability at $C = 3.000142$. The family ends at $C = 3.000147$ on a simple period bifurcation of the

unstable planar orbit shown in the right plot Fig. 14, which clearly impacts Enceladus (equatorial radius ~ 256 km).

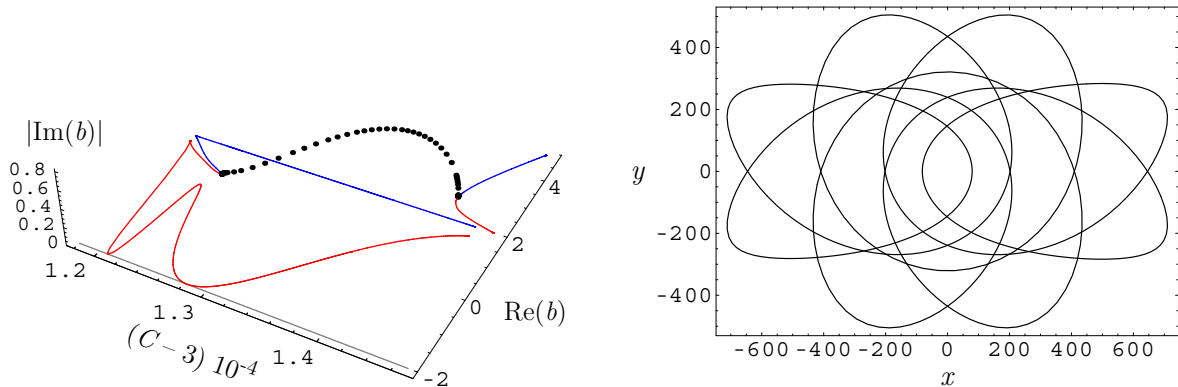


Figure 14.— Left: stability curves of the 9:2 vertical family of the Saturn-Enceladus system. Right: termination orbit (distances are km).

In the region of stability that occurs after the reflection, the orbits remain relatively close to Enceladus and provide global surface coverage, including visibility on every pass of the south pole region where the suspected H_2O plume originates [4]. Figure 15 shows two orbits of this family: an egg-shaped, non impact orbit with very mild instability, and a stable orbit that could be useful as a science orbit.

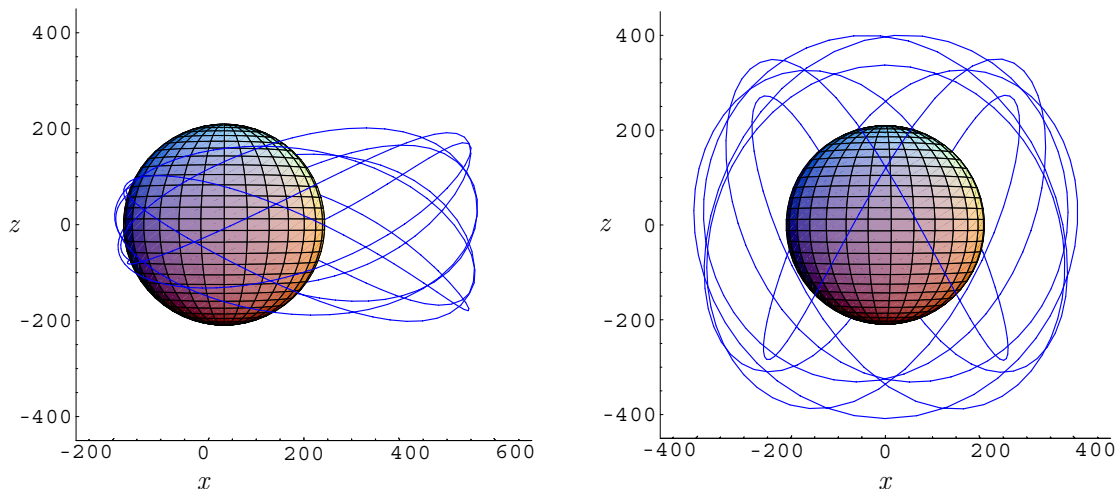


Figure 15.— Non impact periodic orbits around Enceladus (distances are km). Left: Egg-shaped orbit for $C = 3.000139$. Right: stable, science orbit for $C = 3.000118$.

3 Conclusions

The numerical continuation of the family g for different mass ratios between the primaries shows two typical behaviors of the periodic orbits. For $\mu > 0.11$ the almost circular, direct, periodic orbits around the smaller primary are (mildly) unstable in a region between two consecutive reflections of the family. At $\mu \approx 0.11$ the mild instability region

collapses to a critical point of the horizontal stability curve that is neither a reflection nor a bifurcation orbit. For smaller values of μ which widely apply to the solar system dynamics, this region of mild instability disappears.

The computation of different families of periodic orbits that bifurcate vertically from the family g provides regions of stability of three-dimensional motion around the smaller primary that are new, to our knowledge, and could have practical implications. Notably, there exist three-dimensional connections between different phases of planar, direct motion that extend the stability of three-dimensional, oval-shaped, periodic orbits to values of the Jacobi constant where the planar orbits are clearly unstable. These kinds of connections are always found for the computed families for different values of the mass parameter even in Hill's limiting case, which corroborates the view that the different classes of planar, oval-shaped periodic orbits that exist close to the smaller primary belong to the same family g .

Finally, the precise continuation of the mild instability loop of the family g for values of μ close to the critical value of the cusp point challenges numerical continuation algorithms and may be used by researchers as a strong validation test for numerical continuation procedures.

Acknowledgement

M. L. thanks partial support from projects ESP-2004-04376 and ESP-2005-07107 of the Spanish Government.

References

- [1] Broucke, R.A., *Periodic Orbits in the Restricted Three-Body Problem With Earth-Moon Masses*, NASA-JPL TR 32-1168, February 1968 (100 pages).
- [2] Broucke, R.A., "Stability of Periodic Orbits in the Elliptic Restricted Three-Body Problem," *AIAA Journal*, Vol. 7, No. 6, 1969, pp. 1003–1009.
- [3] Darwin, G.H., "Periodic Orbits," *Acta Mathematica*, Vol. 21, 1897, p. 99–243.
- [4] Hansen, C.J., Esposito, L., Stewart, A.I.F., Colwell, J., Hendrix, A., Pryor, W., Shemansky, D., West, R., "Enceladus' Water Vapor Plume," *Science*, Vol. 311, No. 5766, pp. 1422–1425.
- [5] Hénon, M., "Exploration Numérique du Problème Restreint. I. Masses égales, Orbites périodiques," *Annales d'Astrophysique*, Vol. 28, No. 2, 1965, pp. 499–511.
- [6] Hénon, M., "Exploration Numérique du Problème Restreint. II.— Masses égales, stabilité des orbites périodiques," *Annales d'Astrophysique*, Vol. 28, No. 2, 1965, pp. 992–1007.

- [7] Hénon, M., “Numerical Exploration of the Restricted Problem. V. Hill’s Case: Periodic Orbits and Their Stability,” *Astronomy and Astrophysics*, Vol. 1, 1969, pp. 223–238.
- [8] Hénon, M., “Vertical Stability of Periodic Orbits in the Restricted Problem. I. Equal Masses,” *Astronomy and Astrophysics*, Vol. 28, 1973, pp. 415–426.
- [9] Hénon, M., “Vertical Stability of Periodic Orbits in the Restricted Problem. II. Hill’s case,” *Astronomy and Astrophysics*, Vol. 30, 1974, pp. 317–321.
- [10] Lam, T., Whiffen, G.J., “Exploration of Distant Retrograde Orbits around Europa,” paper AAS 05-110, presented at the 15th Spaceflight Mechanics Meetings, Copper Mountain, Colorado, January 2005.
- [11] Lara, M., and San-Juan, J.F., “Dynamic Behavior of an Orbiter Around Europa,” *Journal of Guidance, Control and Dynamics*, Vol. 28, No. 2, 2005, pp. 291–297.
- [12] Lara, M., Russell, R.P., Villac, B., “Classification of the distant stability regions at Europa,” *Journal of Guidance, Control, and Dynamics*, **in press** (2006).
- [13] Lara, M., Russell, R.P., “On the computation of a science orbit about Europa,” *Journal of Guidance, Control, and Dynamics*, Vol. 30, No. 1, 2007, pp. 259–263.
- [14] Michalodimitrakis, M., “Hill’s problem: families of three-dimensional periodic orbits (Part I),” *Astrophysics and Space Science*, Vol. 68, 1980, pp. 253–268.
- [15] Russell, R.P., “Global Search for Planar and Three-dimensional Periodic Orbits Near Europa,” *Journal of the Astronautical Sciences*, **accepted for publication** (2006).
- [16] Szebehely, V., *Theory of Orbits — The Restricted Problem of Three Bodies*, Academic Press, New York, 1967.

Appendix

Equations of motion of the Circular Restricted Three-body Problem

In a synodic system with the origin at the smaller primary and the bigger one to the left of the origin (negative x axis direction), the equations of motion of the Circular Restricted Three-body Problem are

$$\ddot{x} - 2\dot{y} = \Omega_x, \quad \ddot{y} + 2\dot{x} = \Omega_y, \quad \ddot{z} = \Omega_z, \quad (1)$$

where the potential function is $\Omega = (1/2)[(x+1-\mu)^2 + y^2] + (1-\mu)/\rho + \mu/r$, μ is the ratio mass of the smaller primary to the total mass of the system, and ρ and r are the distances to the bigger and smaller primaries respectively $\rho^2 = (x+1)^2 + y^2 + z^2$, $r^2 = x^2 + y^2 + z^2$. The transformation to the barycentric origin is made by a simple translation along the x axis.

Equations (1) accept the Jacobi integral $2\Omega - (\dot{x}^2 + \dot{y}^2 + \dot{z}^2) = C$, where C is known as the Jacobi constant.

Linear stability definitions

The stability of a periodic orbit is derived from the eigenvalues of the state transition matrix at the end of one period, which appear in reciprocal pairs $(\lambda, 1/\lambda)$ in Hamiltonian systems. As periodic orbits enjoy one trivial eigenvalue $\lambda_0 = 1$, periodic orbits of Hamiltonian systems with three degrees of freedom have 4 non-trivial eigenvalues. Then, two stability indices $b_i = \lambda_i + 1/\lambda_i$ ($i = 1, 2$) are normally used, where the condition $b_{1,2}$ real and $|b_{1,2}| < 2$ applies for linear stability.

For planar motions, one index measures the “horizontal” or in-plane stability (that we note b_h), whereas the other (noted b_v) shows the “vertical” stability character of the periodic orbit. At critical values of the stability indices (some non-trivial eigenvalues taking the value $\lambda = \pm 1$) new families of periodic orbits can bifurcate from the original one, either in the plane ($b_h = \pm 2$) or orthogonal to it ($b_v = \pm 2$).

The representation of the stability indices versus the parameter generator of a family of periodic orbits results in stability curves where the changes in the stability of a family can be noted. The stability curves are usually represented in the real plane, but unstable orbits with complex eigenvalues out of the unit circle have complex stability indices.

Bifurcations of families of periodic orbits are not limited to the critical cases $b = \pm 2$. For $-2 < b < 2$ new families of periodic orbits may bifurcate from the original one with multiple period. Thus, for eigenvalues λ that are n -th roots of the unity the stability index is $b = 2 \cos(2\pi d/n)$. A bifurcation orbit with $b = +2$ results after n -periods.